

Can LSTM outperform volatility-econometric models?

German Rodikov^{1,*} and Nino Antulov-Fantulin²

¹Affiliation, SNS, Pisa

²Affiliation, ETH, Zürich

*e-mail: german.rodikov@sns.com, germanrodikov@gmail.com

ABSTRACT

Volatility prediction for financial assets is one of the essential questions for understanding financial risks and quadratic price variation. However, although many novel deep learning models were recently proposed, they still have a "hard time" surpassing strong econometric volatility models. Why is this the case? The volatility prediction task is of non-trivial complexity due to noise, market microstructure, heteroscedasticity, exogenous and asymmetric effect of news, and the presence of different time scales, among others. In this paper, we analyze the class of long short-term memory (LSTM) recurrent neural networks for the task of volatility prediction and compare it with strong volatility-econometric models.

1 Introduction

Although the first stochastic mathematical models of price changes, also known as Brownian motion or Wiener process, were proposed a long time ago ^{1,2}, they still did not fully describe empirical facts ³ connected to the quadratic variation and thus volatility of asset prices. In financial markets, volatility is associated with the level of price fluctuations.

Volatility changes over time; high volatility means high risk and sharp price fluctuations, while low volatility refers to smooth price changes ^{4,5}. For derivative financial instruments, the price is directly referred to as underlying assets (implied) volatility. Thus, it plays a crucial role in these financial instruments. Options and Derivatives have increased in volume over the past decades ⁶. Derivative contracts are written based on volatility measurement. In other words, volatility is the underlying asset. Thus, we can understand why so many researchers and practitioners focus on the volatility model and mostly on forecasting volatility models.

Some models are characterizing the volatility from a conditional process perspective, for example, ARCH family ^{4,5}. The main idea of the conditional process perspective is the use of conditional variance, the values of which change over time, while the unconditional variance can remain relatively constant. The drawback of autoregression models for conditional heteroscedasticity is accuracy performance. Moreover, comparing and evaluating models is difficult because volatility cannot be directly observed. Thus, an additional factor is an approach to determining and calculating volatility.

Stochastic volatility models are expressed as a stochastic process, which means that the volatility value at time t is latent and unobservable ⁷. On the other hand, some models try to estimate it as a non-parametric task, which implements more state freedom in parameter map conditions ^{8,9}. However, non-parametric models did not show outperformance compared to more mainstream approaches.

On the other hand, Neural Networks (NN) has been widely used for forecasting tasks, such as stock prices ¹⁰ or volatility predictions with additional input ¹¹. Some other works focus on combination conditional volatility models with NN ¹². This spectrum of work shows mixed performance results referring to volatility prediction tasks. In some cases were shown that non-parametric models, including NN, present poor forecasting performance for an out-of-sample test ^{13,14}. In ¹⁵ were shown that the feed-forward NN approximation is not well enough. Furthermore, ¹⁵⁻¹⁷ demonstrate mixed forecasts accuracy on out-of-sample realized volatility by NN. However, in ^{17,18} were provided promising results for realized volatility forecasts out-of-sample accuracy. Implied volatility and realized volatility forecasting task were investigated in ¹⁹ was shown that NN performance as well as realized volatility.

Also, in recent decades, there has been an increase in activity in finance using machine learning to detect anomalies and volatility prediction tasks with NLP analysis. The advantage of machine learning is that we do not need to specify the functional form a priori, but rather learn it from data. However, these approaches have not shown substantial benefits in predicting realized volatility w.r.t. standard econometric volatility models. One possibility is that the asymmetrical influence of news on the volatility process ^{20,21} makes it particularly challenging to estimate the structure of the volatility process.

The problem with recurrent neural networks (RNN) is that distant memory of the first entries gradually disappears. After

some iterations, the state of the RNN contains practically no traces of the first entries. For example, each long short-term memory (LSTM) cell defines what to remember, forget, and update memory using gateways. Thus, the LSTM network solves the problem of exploding or disappearing gradients. However, LSTM uses a large number of training parameters and therefore uses more resources. One of the difficulties is incorrectly choosing the optimal number of parameters when dealing with large sequences and caring about accuracy. In this work, we studied and analyzed how Neural Networks (LSTM) can learn to capture the temporal structure of realized volatility. We aim to demonstrate how NN could be used for accurate volatility forecasting. For this purpose, we implement modern Neural Networks, Long Short Term Memory (LSTM)²², and the successor (next generation) of LSTM, Gated Recurrent Unit (GRU)²³. Machine learning can approximate any linear and non-linear behavior and could learn data structure. However, hyper-parameters of NN could lead to different results. However, preprocessing of data and the combining procedure could be essential elements to achieve good performance. We investigated the approach with LSTM and GRU types for realized volatility forecasting tasks and compared the predictive ability of NN with widely used EWMA, HAR, GARCH-family models.

The remaining of the paper is organized as follows. Section 2 provides some preliminaries, such as the definition of realized volatility, showing some factors, for instance, data frequencies of time series. Section 3 introduces all benchmarks and models for comparisons. Section 4 describes the NN architecture, data, methodology, and choice and reveals critical factors for such performance. Section 5 lists the analysis of forecast performance and evaluation for our models. Finally, the technical specification of all models is listed in Appendix.

2 Preliminaries

Simulations of stocks are often modeled using stochastic differential equations (SDE). Because of the randomness associated with stock price movements, the models cannot be developed using ordinary differential equations (ODE). A typical model used for stock price dynamics is the following stochastic differential equation:

$$dS = \mu S dt + \sigma S dW_t, \quad (1)$$

where S is the stock price, μ is the drift coefficient or mean of returns over some time period, σ is the diffusion coefficient or the standard deviation of the same returns, and W_t is known as the Wiener process or Brownian Motion.

Each increment W_i is computed by multiplying a standard random variable z_i from a normal distribution $N(0, 1)$ with mean 0 and standard deviation 1 by the square root of the time increment $\sqrt{\Delta t_i}$:

$$W_i = z_i \sqrt{\Delta t_i}. \quad (2)$$

The cumulative sum of the W_i increments is the discretized path:

$$W_n(t) = \sum_{i=1}^n W_i(t) \quad (3)$$

For the SDE Equation 3 with an initial condition for the stock price of $S(0) = S_0$, the closed-form solution of Geometric Brownian Motion (GBM) is

$$S(t) = S_0 e^{(\mu - \frac{1}{2}\sigma^2)t + \sigma W_t} \quad (4)$$

Usually, stock prices volatility changes stochastically over time, but in GBM, volatility is assumed constant. In an attempt to make it practical as a model for stock prices, assumption that the volatility σ is constant. A local volatility model could be derived from volatility as a deterministic function of the stock price and time. However, we assume that the volatilities randomness is own and often described by a different equation driven by a different Wiener process; the model is called a stochastic volatility model. The Black-Scholes-Merton model assumes that volatility is constant. In practice, volatility varies through time, and a lognormal distribution of price will be obtained in the future²⁴. We could consider processes, for instance, retaining the property of continuous change in the price of an underlying asset but assuming a process other than geometric Brownian motion. Also, another alternative is to superimpose continuous changes in asset prices in leaps and bounds. Another alternative is to assume a process in which all asset price changes are jumped. The types of processes are collectively known as Levy processes²⁵. In general, we could also consider the Levy process, as implemented as a continuous-time stochastic process

but with stationary independent increments. But let's suppose first that the volatility parameter in the Geometric Brownian motion is a known function of time, the process followed by the asset price then:

$$dS = \mu S dt + \sigma(t) S W_t \quad (5)$$

It was shown that²⁴, when volatility is stochastic but uncorrelated with the asset price, the price could be described by Black-Scholes-Merton integrated over the probability distribution of the average variance rate. The case where the asset price and volatility are correlated is more complicated, and in this perspective, we should consider the model with two stochastic variables, price, and volatility.

In this paper, we will be focusing on the realized volatility of a particular asset. Let us denote the log-price of asset at time t as $p(t)$. Furthermore, intra-day return with for a given segment j and frequency Δ is $r_{t-j*\Delta} = p_{t-j*\Delta} - p_{t-(j+1)*\Delta}$. Then, the daily realized volatility is defined as the square root of the sum of intra-day squared returns

$$RV_t^d = \sqrt{\sum_{j=0}^{M-1} r_{t-j*\Delta}^2} \quad (6)$$

Next, the realized volatility (RV) is the consistent estimator²⁶ of the squared root of the integrated variance (IV). There is even a more robust result²⁷ stating that RV is a consistent estimator of quadratic variation if the underlying process is a semimartingale. The integrated one-day variance (IV) at day t is defined as

$$IV_t^d = \int_t^{t-1d} \sigma^2(\omega) d\omega \quad (7)$$

The measurement is set by the specification for each case separately. For instance, the calculation could be done for realized volatility of daily returns over one month, or the realized volatility could be calculated on returns of minutes level per one day. However, taking into account a time frame of less than 1-5 minutes could be complicated by noise⁵.

Underlying processes and parameters are time-varying. There could be various shapes of returns distributions^{4,5,20,21}. It may hamper the estimation of volatility and assessment of the underlying process. Consider σ as a risk measure, which has drawbacks if we do not have a distribution or pricing dynamic. On the other hand, if we consider σ as an uncertainty measure, we should consider a normal distribution for the returns⁶.

More investigated stylized volatility facts are fat tails, volatility clustering, leverage effects, long memory^{20,25,28-30}. Stylized volatility facts have important implications for predicting volatility³¹. Given these patterns, volatility models have been designed in different ways.

3 Models and Benchmarks

This section aims to show various widely used models in measuring and forecasting volatility. We are focusing on models which primarily developed based on historical behavior and did not take into account additional input as news, market microstructure data, or macroeconomic rates³².

We do not consider any classical non-parametric model, and it was demonstrated^{6,8,9} that non-parametric methods' accuracy is not high enough.

3.1 GARCH-family models

GARCH family models estimate historical volatility or conditional variance⁵; the autoregressive conditional heteroskedasticity (ARCH)⁴ model is defined by

$$\begin{cases} r_t = \mu + \sigma_t \varepsilon_t \\ \sigma_t^2 = \alpha_0 + \sum_{i=1}^q \alpha_i (r_{t-i} - \mu)^2 \end{cases} \quad (8)$$

Where $\varepsilon_t \sim \mathcal{N}(0, 1)$ and $\sigma_t \varepsilon_t \sim \mathcal{N}(0, \sigma_t^2)$. Conditional variance refers to a linear function of the past conditional variance, but volatility is a deterministic function of historical returns. In⁵ generalized the ARCH model by modeling the variance as an AR(p), GARCH-model estimates future volatility from a long-run variance, and recent variance estimation.^{5,33}. Thus, the clustering effect is a sharp increase of volatility observed for some time and not followed by a sharp drop.

$$\sigma_t^2 = \omega + \alpha * r_{t-1}^2 + \beta * \sigma_{t-1}^2, \quad \omega > 0, \alpha > 0, \beta > 0 \text{ and } \gamma + \alpha + \beta = 1 \quad (9)$$

Various extensions have been intruded since Exponential GARCH³⁴, GJR-GARCH³⁵, and Threshold GARCH³⁶ in this model encapsulating some of the stylized facts about volatility. Among the multiple models of the GARCH family, the GARCH(1,1) model is the most popular³⁷. However, the complication and increase in the order of the model do not lead to more significant results but complicate the calculations³⁸.

Although the GARCH process is driven by a single noise sequence, the diffusion is driven by two independent Brownian motions

$$\left(W_t^{(1)} \right)_{t \geq 0} \text{ and } \left(W_t^{(2)} \right)_{t \geq 0} \quad (10)$$

For example, the GARCH(1, 1) diffusion satisfies³⁹:

$$\begin{cases} dS_t = \sigma_t dW_t^{(1)} \\ d\sigma_t^2 = \theta (\gamma - \sigma_t^2) + \rho \sigma_t^2 dW_t^{(2)}, \quad t \geq 0 \end{cases} \quad (11)$$

The behavior of this diffusion limit is therefore rather different from that of the GARCH process itself since the volatility process $(\sigma_t^2)_{t \geq 0}$ evolves independently of the driving process $(W_t^{(1)})_{t \geq 0}$ in the first of the equations.

3.2 Heterogeneous Autoregression Realized Volatility

The heterogeneous Autoregression Realized Volatility (HAR-RV) model introduced by⁴⁰ is based on the assumption that agents' behavior in financial markets, according to which they differ in their perception of volatility depending on their investment horizons and are divided into short-term, medium-term and long-term. The hypothesis of the existence of such heterogeneous structures in financial markets is based on the heterogeneous market hypothesis presented by⁴¹.

Different agents in a heterogeneous market have different investment periods and participate in trading on the exchange with different frequencies. The fundamental idea is that participants' basic decisions on different time horizons perceive and respond to different types of volatility. Suppose we assume that the memory of each component (the rate of decrease of the values of the autocorrelation function with an increasing lag) is exponentially decreasing with a particular time constant. In that case, the memory of the entire market will consist of many such exponentially decreasing components with various values of time constants. Moreover, their superposition will behave like a process with hyperbolically decreasing autocorrelation.

So, a short-term agent may react differently to fluctuations in volatility compared to a medium- or long-term investor. The HAR-RV model is an additive cascade of partial volatilities generated at different time horizons that follows an autoregressive process. Log realized volatilities in using the HAR-RV⁴⁰ given the lognormal distribution. Thus, the HAR-RV approach is one more stable and accurate estimate for Realized Volatility⁴². We worked with logs to avoid negativity issues and get approximately Normal distributions, consider the log RV_t aggregated, as follows:

$$\log RV_t^{(n)} = \frac{1}{n} (\log RV_t + \dots + \log RV_{t-n+1}) \quad (12)$$

at the 3 different horizons, where $RV_t^{(d)}$, $RV_t^{(w)}$, and $RV_t^{(m)}$ are respectively the daily, weekly, and monthly observed realized volatilities.

$$\begin{cases} \tilde{\sigma}_{t+1m}^{(m)} = c^{(m)} + \phi^{(m)} RV_t^{(m)} + \tilde{\omega}_{t+1m}^{(m)} \\ \tilde{\sigma}_{t+1w}^{(w)} = c^{(w)} + \phi^{(w)} RV_t^{(w)} + \gamma^{(w)} \mathbb{E}_t \left[\tilde{\sigma}_{t+1m}^{(m)} \right] + \tilde{\omega}_{t+1w}^{(w)} \\ \tilde{\sigma}_{t+1d}^{(d)} = c^{(d)} + \phi^{(d)} RV_t^{(d)} + \gamma^{(d)} \mathbb{E}_t \left[\tilde{\sigma}_{t+1w}^{(w)} \right] + \tilde{\omega}_{t+1d}^{(d)} \end{cases} \quad (13)$$

where $c^{(m)}$ - the constant and $\tilde{\omega}_{t+1m}^{(m)}$ is an innovation that is simultaneously and consistently independent with a mean zero, for monthly aggregation. By straightforward recursive substitution of three factors Stochastic Volatility model where the factors are directly the past RV:

$$\log \sigma_{t+1d}^{(d)} = c + \beta^{(d)} \log RV_t^{(d)} + \beta^{(w)} \log RV_t^{(w)} + \beta^{(m)} \log RV_t^{(m)} + \varepsilon_{t+1d}^{(d)}. \quad (14)$$

And we could add a measure of errors ε for log RV:

$$\log \sigma_{t+1d}^{(d)} = \log \text{RV}_{t+1d}^{(d)} + \tilde{\varepsilon}_{t+1d} \quad (15)$$

Therefore autoregression model in the RV with the feature of considering volatilities realized over different interval sizes:

$$\log \text{RV}_{t+1d}^{(d)} = c + \beta^{(d)} \log \text{RV}_t^{(d)} + \beta^{(w)} \log \text{RV}_t^{(w)} + \beta^{(m)} \log \text{RV}_t^{(m)} + \varepsilon_{t+1d} \quad (16)$$

3.3 Autoregressive Integrated Moving Average

A feature of the time series for the Autoregressive Integrated Moving Average (ARIMA) application lies in the relationship between past values associated with current and future ones. Therefore, ARIMA models allow modeling integrated or differential-stationary time series. ARIMA's approach to time series is that the stationarity of the series is assessed first. Next, the series is transformed by taking the difference of the corresponding order, and some ARMA model is built for the transformed model⁴³.

Box-Jenkins ARIMA (an integrated autoregressive moving average model) models are widely used for time series modeling. The models are autoregressive models (AR), and moving average (MA) models. Let y_t be a stationary time series that is the realization of a stochastic process. The general ARMA(p,q) model:

$$y_t = \sum_{i=1}^p \phi_i y_{t-i} + a_t - \sum_{j=1}^q \theta_j a_{t-j} \quad (17)$$

where a_{t-j} is errors or residuals that are assumed to follow a normal distribution. When the time series exhibits nonstationary behavior, then the ARMA model can be extended and written using the differences:

$$W_t - \sum_{k=1}^d W_{t-k} = (1-B)^d Y_t \quad (18)$$

where d is the order of the difference. Replacing the ARMA model with the differences in eq. gives us:

$$\phi_p(B)(1-B)^d Y_t = \theta_q(B) a_t \quad (19)$$

the ARIMA model (p, d, q), where p is autoregressive order of AR(p), d - order of integration (differences of the original time series) and q order of the moving average MA(q). The weakness of ARIMA models is the inability to model volatile variance. Since this type of variance is very common in currency pairs, persistent volatility cannot capture some of the basic properties of heteroscedastic volatility present in financial time series, such as stochastic volatility, clustering volatility, mean reversion, and fat tails.

3.4 Moving average and exponential moving average

Exponential volatility also represents random returns like a normal distribution. The peculiarity of this method of calculating volatility is that when calculating the standard deviation, the historical sample data are included in the calculation with weights that increase the weight of recent price movements in the sample compared to long-term actions. Exponentially Weighted Moving Average (EWMA) corrects simple variance problems by weighting individual periodic returns and giving more weight to recent observations. This method is a pretty good benchmark, along with a naive approach.

$$\text{EWMA}(\sigma_n^2) = \alpha \sigma_{n-1}^2 + (1 - \alpha) R_{n-1}^2 \quad (20)$$

3.5 LSTM and GRU

A neural network could be imaged as a layered structure of connected neurons. Recurrent neural networks (RNN) are a class of NN that use previous outputs as inputs. Due to this, Recurrent neural networks could work with sequential data. RNN neurons have cell state/memory, and input is processed according to this internal state, achieved by this recurrent mechanism. In RNNs,

there are repeating activation modules of layers that allow them to store information, but not enough. However, RNNs often suffer from a vanishing gradient, which causes model training to become too slow or stop altogether.

LSTM is a specific cell type in a recurrent neural network capable of catching long-term dependencies in data and fixing this exploding or vanishing gradient issue. Achievement is possible due to cell state and a combination of four gates interacting. The ability to eliminate or add information to the cell state, carefully regulated by gates structures, is a crucial difference with RNN. LSTM cells contain an additional state, which helps to internally maintain input memory, making them especially suitable for solving problems associated with sequential. Cell state conveys relative information along the entire chain of the sequence. The state of the cell reflects the corresponding information throughout the processing of the series, so data from earlier time steps can participate in later time steps⁴⁴.

$$f_t = \sigma(W_f \cdot [h_{t-1}, x_t] + b_f) \quad (21)$$

$$i_t = \sigma(W_i \cdot [h_{t-1}, x_t] + b_i) \quad (22)$$

$$\tilde{C}_t = \tanh(W_C \cdot [h_{t-1}, x_t] + b_C) \quad (23)$$

$$C_t = f_t * C_{t-1} + i_t * \tilde{C}_t \quad (24)$$

$$o_t = \sigma(W_o \cdot [h_{t-1}, x_t] + b_o) \quad (25)$$

$$h_t = o_t * \tanh(C_t) \quad (26)$$

GRU is a new generation of recurrent neural networks, very similar to LSTMs, a variation on the LSTM, introduced in⁴⁵. The update gate combines the forget and input gates, and the cell state merges with the hidden state called the reset gate. As a result, the model is more straightforward, and the training procedure takes less time than the net with standard LSTM instead of GRU. By this modification, LSTM and GRU fix the vanishing/exploding gradient problem encountered by traditional RNN

$$z_t = \sigma(W_z \cdot [h_{t-1}, x_t]) \quad (27)$$

$$r_t = \sigma(W_r \cdot [h_{t-1}, x_t]) \quad (28)$$

$$\tilde{h}_t = \tanh(W \cdot [r_t * h_{t-1}, x_t]) \quad (29)$$

$$h_t = (1 - z_t) * h_{t-1} + z_t * \tilde{h}_t \quad (30)$$

Constructing a neural network is carried out by enumeration and finding the architecture with a minor error. In⁴⁶ provided definitions of information criteria that can assist in defining a neural network. Nevertheless, learning different architectures and choosing by mistake remains the most commonly used.

4 Experiments

4.1 Accuracy measures

The Mean Squared Error method minimizes the sum of the squared deviations of the actual values from the calculated sum of squared errors. If this sum is divided by the number of observations, we get MSE.

If the MSE did not have a power of 2, then the positive and negative deviations would cancel out, which would minimize the distance between the actual and calculated values. Thus, the presence of squares allows getting some estimate of the distance from the actual values to the line.

$$\text{MSE} = \frac{1}{n} \sum_{i=1}^n (Y_i - \hat{Y}_i)^2 \quad (31)$$

For Mean Absolute Error, allow to get rid of signs and estimate the distance from the actual to the calculated values, which will need to be minimized. The undoubted advantage of MAE is that the modules do not multiply the deviations that are

considered outliers. Therefore, this estimate is more robust than MSE.

$$\text{MAE} = \frac{\sum_{i=1}^n |Y_i - \hat{Y}_i|}{n}, \quad (32)$$

where a test data sample has n data points, Y_i is the observed values of the predicted variable and \hat{Y}_i the predicted values. Also, we provide the result of the Root Mean Squared Error, which is just the square root of MSE; the Mean Absolute Percentage Error (MAPE) is measured percentage accuracy.

4.2 Diebold-Mariano test

The Diebold-Mariano test⁴⁷ compares the forecast accuracy of two forecast models. In⁴⁸ were addressed the finite sample properties of the Diebold-Mariano statistics. The additional assumption is that all autocovariance beyond some lag length is zero and modified test based on an approximately unbiased estimator. The null hypothesis - the two models have equal forecast accuracy. However, the alternative hypothesis is that model 2 is less accurate than model 1. The alternative hypothesis is that model 2 is more accurate than model 1. Also, we could make two sides alternative hypotheses: method one and method 2 have different levels of accuracy.

4.3 Value at Risk

Value at Risk (VaR)⁴⁹ is a monetary estimate of the amount that the expected loss over a given period will not exceed with a given probability. VaR is the amount of losses on the investment portfolio for a fixed period if some adverse event occurs that may affect the market. As a time horizon, usually, one, five, or ten days is chosen since it is complicated to predict the behavior of the market for a more extended period. The level of acceptable risk is taken equal to 95 or 99 percent.

4.4 Data

This study analyzes how NN could estimate and predict realized volatility on different market structures, particularly indexes, stocks, and cryptocurrency. Also, we consider different time frames and analyze the effect and dependencies of data granularity Table 1.

For **stock market data** for each day, we calculate RV based on the 1-minute time frame price observations. But returns are calculated on the last daily close price. As a result, our experimental data set is the table of intraday returns and corresponded Realized Volatility. The dataset was divided into three parts: training, validation, and test. The validation and the test sample of stocks are equivalent to 252 points that refer to the trading year.

In the next part, we consider the **S&P 500 index**. We investigated the dataset corresponding to a daily time frame price of S&P 500, in total 17923 price data points to calculate 815 RV observation points, calculation analogous to stocks. However, for this case, we calculated monthly Realized Volatility based on days log-returns instead of stocks data daily RV based on a 1-minute time frame. For the validation data set, and the test set we used 245 data points.

In the last part of our experiment, we investigated **cryptocurrency data**, particularly Bitcoin-USD and Ethereum-USD cryptocurrency pairs. We had prices of Bitcoin corresponding to a 1-minute time frame, however, Ethereum was taken from a high-frequency data frame corresponding to a seconds time frame. The cryptocurrency data was divided into three parts: training, validation, and test similar to stock and index data. The validation and the test sample are the exact sizes of the stock data set validation, and the test set 252 points.

Type of asset	Name	Time frame	From	To	Price points	RV points	Aggregation
Stock	Citigroup Inc.	1-minute	02-Jan-98	28-Apr-17	2309304	4862	day
Stock	Dell T. Inc.	1-minute	02-Jan-98	29-Oct-13	1730585	3982	day
Stock	CBS Inc.	1-minute	02-Jan-98	25-Oct-13	1730411	3980	day
Index	S&P500	1-day	01-Feb-50	01-Dec-17	17923	815	month
Cryptocurrency	Bitcoin-USD	1-minute	31-Dec-11	22-Apr-20	4363457	3035	day
Cryptocurrency	Ethereum-USD	1-second	01-Feb-20	21-May-20	8237492	2650	hour

Table 1. Description of the data for stock, index and cryptocurrency.

4.5 Hyperparameter Optimization and Data Preprocessing

We explored different configurations in terms of dynamic and objective outcomes, and it is a trial and test way to explore the best setups for a given task. To find the best configuration of NN is necessary to conduct multiple experiments with different

hyperparameters⁴⁶. Therefore, we set up and interpreted the results of many training epochs and chose an appropriate one by the low Equation 31 and Equation 32 metrics for the validation data set. In this paragraph, we list the hyperparameters of the experiments for LSTM. Layers and neurons: by implementing different settings we could archive specific types of estimation and deep structure. Loss Function: MSE, MAE, and Huber - different loss functions could lift performance. Activation function: determines how the weighted sum of the input is converted to output. Batch size: the hyperparameter that refers to the number of training examples used per iteration. Epochs: a number that determines how much interaction the learning algorithm runs throughout the learning process. Optimizer: play a critical role in improving model accuracy. There were various options to be used, but the fastest optimizers do not usually achieve higher accuracy. We performed a standard LSTM model with hyperparameter optimization and introduced a window size optimization approach.

Hyperparameters	Values
Window size	[1-50]
Layers	[1-5]
Units in layers	[5,10,20,30,50,100,200]
Dropout	[0.01, 0.05, 0.1, 0.2, 0.3]
Activation fn	[linear, ReLU, SoftMAX, Tanh]
Loss fn	[MAE, MSE, HUBER]
Epochs	[1,2,3,4,5,10,20,30,50,100,1000]
Batch size	[1,2,4,8,16,32,64,128]
Optimizer	[RMSprop, SGD, ADAM]

Table 2. The Table of LSTM Hyperparameters

LSTM has a state layer C_t , practically C_t helps LSTM capture long dependency besides length input. LSTM should be effective for any reasonable length. However, a correctly defined window length is a crucial parameter for this task to show high accuracy. Worth noticing, if we look at HAR or ARIMA models, we have to define lag. How long the series contains the necessary data to forecast the next prediction horizon. However, it should be taken into account that when we differentiate price data, we vanish some of the data properties (since it is contained in the price) to obtain stationary series. Perhaps this is the critical feature why LSTM can achieve such results since a series with a length of n lags is kept due to the cell memory mechanism⁵⁰. We implemented LSTM with a high-level neural network API Keras, which is written in Python and running on top of TensorFlow⁵¹.

We used the following settings to train LSTM: we use as input $(RV_{t-n}, \dots, RV_{t-1})$ and RV_t as target variable, we constructed our prediction task as an autoregression problem. In our experiment, autoregression showed more promising results than regression, which could be described as $RV_t \sim \alpha P_t + \varepsilon_t$.

Another important hyperparameter is the activation function. There is a lack of experiments that consider different activation functions and performance for volatility prediction tasks. There are several possible variants we thought had more potential for our objective Table 2. Moreover, another vital hyperparameter is an optimizer, commonly implemented ‘adam’ optimizer not always suited for all tasks. Nevertheless, as we have shown further, proper choosing functions and optimizers could make a significant difference.

However, the critical element in our experiment was dedicated to exploring the size of the sliding window. Therefore, we did not stop using a window size of n data points; we learned this hyperparameter by LSTM. We do not use augmented by external information approaches.

Moreover, standardization is essential before training LSTM and can often improve the efficiency of training models. Therefore, we implemented an approach for normalizing input data from 0 to 1 by min-max scale.

We also optimized the parameter α of EWMA for MSE and MAE accuracy measures. As well we go through the optimization procedure for the HAR-RV model for MSE and MAE metrics. Nevertheless, we still have the standard model with parameters 1,5,22. In addition, ARIMA GARCH and GJR-GARCH were optimized based on information criteria, as were suggested in⁵².

5 Results

In this empirical study, we sought to unravel the following questions. First, how do configurations of LSTM RNN (number of layers and neurons, activation functions, optimizer) network influence forecasting? Could hyperparameter optimized LSTM outperform the leading models in the field? How much does the sliding window size affect LSTM efficiency and the model performance if this stage is excluded?

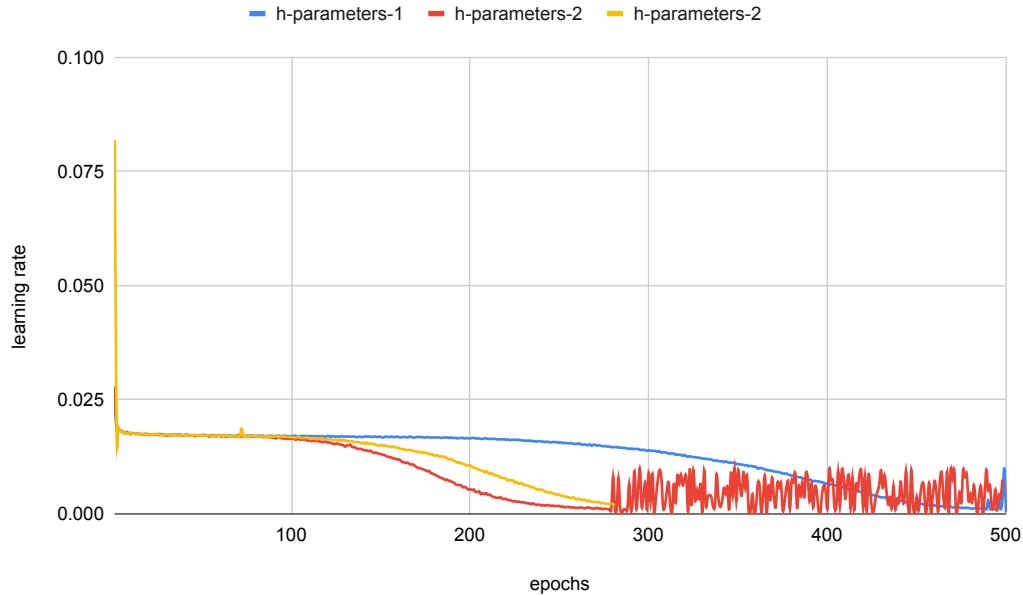


Figure 1. Learnign process of LSTM with different hyperptaratenes

In this section, we want to provide results for three different types of data sets we considered in our experiment: stocks, index, and cryptocurrency, and for three different aggregations of RV monthly, daily, and hourly. We show the performance of the discussed models and detailed comparisons. We performed standard accuracy measures for the one-step-ahead prediction using RMSE, MAE metrics and tested the significance of improvement by the Diebold-Mariano test, Table 3 and the Appendix section.

The best results were demonstrated in the stock market by three types of models: LSTM window, HAR-RV, and EWMA. Interestingly, the LSTM window showed the best accuracy for MAE indicators at all validation samples of stocks. However, for RMSE, HAR hyperparameter optimization often became better, except for the Citi-stock data set, where EWMA was the best. Nevertheless, the out-of-sample RMSE and MAE accuracy-test LSTM with window optimized outperforms other models. DM-test also showed significant accuracy of the forecast quality compared to the closest competitor. According to the MAE out of sample test, the LSTM window optimized model was the best for the Dell stock data set, but HAR had the best RMSE without optimized parameters.

For performance comparison for different market conditions, we investigated the S&P 500 index data set, where the data granularity does not have such extension as the data set of stocks or cryptocurrencies. Therefore, the results obtained should be inverse. On validation, the model could not show the best result, both for RMSE and MAE, although the gap was not significant at 0.1% accuracy, and this was the second most accurate result. However, the LSTM with optimized window showed better accuracy for RMSE with a broad margin accuracy for the out-of-sample result. The DM test also showed the statistical significance of forecast accuracy. This is surprising enough, knowing about the intensity to train a network with a large number of parameters, and the need for large amounts of training data as opposed to econometric models.

LSTM also showed high accuracy performance in the cryptocurrency market, both on the validation and out of sample samples. However, it should be noted that the case of bitcoin out of sample HAR-RV was at the same level. We can trace the tendency that window optimization for LSTM is vital since with more granular data, the window increases.

In the case of high-frequency data, the LSTM with the window-optimized approach shows more stable results. However, the LSTM with a fixed window experienced low-performance accuracy.

6 Conclusion and discussion

This work investigated whether neural networks can capture underlying processes for different markets such as stocks and cryptocurrency markets, gaining popularity in recent years. One of the peculiarities of RNN is that we do not need to know the

parameters of the variable that we are trying to predict, which makes the processing data unified for the stock and cryptocurrency markets. This study used realized volatility as a target variable and formulated experiments as an autoregression problem.

We investigated the sets of hyperparameters for the model and their impact on performance. However, more crucial, we found out that the proper parameter of the rolling window in preprocessing procedure provides a better result in accuracy terms. Furthermore, we found that the more efficient size of the rolling window is from 5 to 12 periods. In this way, LSTM could outperform well-known models in this field, such as HAR-RV. Out-of-sample accuracy tests have shown that LSTM offers significant advantages in both types of markets.

Despite the effectiveness of NN, there are still many difficulties, one of which, for example, is that they are black boxes and do not make it possible to analyze the relationships in the data. This work mainly examined what accuracy can be expected from LSTM in these tasks and what may influence the results. Another obvious problem is the number of parameters to be learned during the training process compared to HAR or EWMA models. On the other hand, modern computing power allows to compute it relatively fast.

Model	MSE (e-05)	RMSE (e-03)	MAE (e-03)	MAPE	DM test MSE	P-value MAE DM	DM test MAE	P-value MAE DM2	VaR 10 days
-------	---------------	----------------	---------------	------	----------------	----------------------	----------------	-----------------------	----------------

Dell Technologies Inc stock - daily aggregation

EWMA MSE	14,1142	11,8803	7,7360	43,3397	0,4295	0,6679	3,6767	0,0002	0,2544
EWMA MAE	13,8962	11,7882	7,5838	41,6260	0,1543	0,8774	3,2005	0,0015	0,2544
HAR MSE	13,7309	11,7178	8,2606	53,1560	-0,0507	0,9595	5,5384	<e-08	0,1533
HAR MAE	13,6397	11,6789	8,2126	52,9801	-0,1722	0,8633	5,5707	<e-08	0,1533
HAR	13,6397	11,6789	8,2126	52,9801	-0,1722	0,8633	5,5707	<e-08	0,1533
Last Values	17,9422	13,3948	7,6268	37,4586	2,3131	0,0215	1,7587	0,0798	0,1383
ARIMA	14,5067	12,0444	7,4324	40,7973	8,7439	<e-08	12,052	<e-08	0,1986
GARCH	79,9334	28,2725	13,720	82,4810	1,6996	0,0904	4,6902	<e-08	0,2040
GJR-GARCH	48,6597	22,0589	11,716	70,0866	1,4385	0,1515	4,1625	<e-08	0,1728
LSTM standart	19,9589	14,1276	9,0725	56,4351	4,7601	<e-08	6,7555	<e-08	0,1196
LSTM window	13,0910	11,4416	6,8530	35,8922	***	***	***	***	0,1280

The Standard and Poor's 500 Index (S&P 500) - monthly aggregation

EWMA MSE	51,7004	22,7377	14,8143	32,0655	3,4105	0,0007	4,3333	<e-08	0,2807
EWMA MAE	47,6968	21,8396	14,0323	30,1342	2,9263	0,0037	2,7277	0,0068	0,2805
HAR MSE	49,4088	22,2281	13,4078	28,1917	2,2882	0,0229	1,7231	0,0861	0,3185
HAR MAE	49,1897	22,1787	13,2569	27,3338	2,2819	0,0233	1,3088	0,1918	0,3177
HAR	45,0559	21,2263	12,7762	26,790	2,5911	0,0101	-0,3437	0,7313	0,3185
Last Values	43,1101	20,7629	14,2981	30,7739	0,2095	0,8341	2,2326	0,0264	0,3525
ARIMA	46,1339	21,4788	14,1858	30,8716	3,0891	0,0022	6,0096	<e-08	0,2823
GARCH	174,268	41,7454	34,1938	71,0463	9,5905	<e-08	18,972	<e-08	0,1040
GJR-GARCH	175,741	41,9215	34,5954	71,9429	9,6029	<e-08	19,613	<e-08	0,1046
LSTM standart	48,7022	23,5619	14,4471	32,9160	3,4729	<e-08	12,181	<e-08	0,1511
LSTM window	41,6775	20,4150	12,8474	28,505	***	***	***	***	0,3374

Ethereum USD cryptocurrency - hourly aggregation

EWMA MSE	14,5095	12,0455	6,4798	26,0383	0,6170	0,5377	1,6013	0,1105	0,2472
EWMA MAE	15,1958	12,3271	6,6222	26,8891	0,5746	0,5660	1,8285	0,0686	0,2469
HAR MSE	13,1807	11,4807	6,6540	29,3306	-0,2493	0,8033	2,2370	0,0261	0,1787
HAR MAE	14,7789	12,1568	7,1052	31,6274	0,7861	0,4325	3,0047	0,0029	0,1813
HAR	13,1785	11,4797	6,6583	29,3342	-0,2573	0,7971	2,2608	0,0246	0,1787
Last Values	16,6921	12,9198	6,9548	28,7158	0,7582	0,4490	2,1630	0,0314	0,1683
ARIMA	15,1794	12,3204	7,3057	31,4821	2,7745	0,0059	7,1878	<e-08	0,1801
GARCH	584,465	76,4503	54,010	239,247	4,6473	<e-08	14,769	<e-08	0,5650
GJR-GARCH	513,573	71,6640	51,818	229,280	5,0685	<e-08	15,610	<e-08	0,5489
LSTM standart	27,5347	16,5935	10,357	37,0491	3,1206	0,0020	10,646	<e-08	0,0946
LSTM window	13,5033	11,6203	6,0079	22,6919	***	***	***	***	0,1461

Table 3. Dell-stock, S&P 500 and ETH-USD out-of-sample, 1-step ahead accuracy test for 252 points.

7 Appendix

Model	Description	Parameters	MSE (e-05)	RMSE (e-03)	MAE (e-03)	MAPE
EWMA MSE	alpha	0,55	5,3717	7,3292	4,8341	24,7917
EWMA MAE	alpha	0,39	5,4270	7,3668	4,8229	24,8157
HAR MSE	d,w,m:	2, 10, 110	5,4438	7,3782	4,9074	26,7506
HAR MAE	d,w,m:	2, 8, 110	5,5006	7,4166	4,8697	26,5904
HAR	d,w,m:	1, 5, 22	5,9750	7,7298	5,1681	28,5730
Last Values	–	–	5,9519	7,7149	4,9908	25,9581
ARIMA	(p,d,q):	(0, 1, 1)	5,5867	7,4744	4,8460	25,2255
GARCH	order	1,1	82,780	28,771	18,711	138,802
GJR-GARCH	order	1,1	148,29	38,509	19,945	138,565
LSTM standart	–	–	8,2386	9,0766	5,2918	22,7666
LSTM window	window	7	5,3780	7,3334	4,5678	22,4754

Table 4. Citi-stock, validation-dataset, 1-step ahead forecast, accuracy for 252 points.

Model	MSE (e-05)	RMSE (e-03)	MAE (e-03)	MAPE	DM test mse	P-value mae DM	DM test mae	P-value mae DM2	VaR 10 days
EWMA MSE	15,7334	12,5432	5,0453	26,0561	1,3554	0,1764	0,2452	0,8064	0,2210
EWMA MAE	14,4100	12,0041	5,0380	26,4374	1,6034	0,1100	0,3089	0,7576	0,2210
HAR MSE	12,8315	11,3276	5,1757	30,3151	0,8969	0,3706	1,6235	0,1057	0,1323
HAR MAE	12,8811	11,3495	5,2473	30,8161	1,0622	0,2891	2,2648	0,0243	0,1324
HAR	13,5329	11,6331	5,3237	30,5739	2,8817	0,0042	2,6992	0,0074	0,1313
Last Values	22,1741	14,8909	5,4230	27,4143	1,1727	0,2420	0,7796	0,4363	0,1237
ARIMA	16,5116	12,8497	5,2158	28,0231	4,7375	<e-08	7,7129	<e-08	0,1380
GARCH	111,245	33,3534	15,949	88,1419	3,1129	0,0020	6,3205	<e-08	0,2257
GJR-GARCH	177,384	42,1170	15,395	76,5359	2,5231	0,0122	4,3916	<e-08	0,2177
LSTM standart	16,2284	12,7390	5,9516	27,5748	3,3236	0,0010	3,2068	0,0015	0,0808
LSTM window	12,4381	11,1526	4,9629	28,6159	***	***	***	***	0,1291

Table 5. Citi-stock, out-of-sample test, 1-step ahead forecast, accuracy for 252 points.

Model	Description	Parameters	MSE (e-05)	RMSE (e-03)	MAE (e-03)	MAPE
EWMA MSE	alpha	0,12	12,3047	11,0926	7,7043	30,4275
EWMA MAE	alpha	0,15	12,3367	11,1070	7,6868	30,1312
HAR MSE	d,w,m:	1, 12, 26	12,0715	10,9870	7,8279	31,8926
HAR MAE	d,w,m:	1, 11, 28	12,1427	11,0194	7,8179	31,8276
HAR	d,w,m:	1, 5, 22	12,3529	11,1143	7,9304	32,2523
Last Values	–	–	20,0029	14,1431	9,3039	34,3112
ARIMA	(p,d,q):	(1, 1, 2)	13,2909	11,5286	8,1161	32,3217
GARCH	order	1,1	105,525	32,4846	23,036	89,3186
GJR-GARCH	order	1,1	105,525	32,4846	23,036	89,3186
LSTM standart	–	–	19,4981	13,9635	9,0714	27,9306
LSTM window	window	8	13,4469	11,5960	6,9357	23,2722

Table 6. Dell-stock, validation-dataset, 1-step ahead forecast, accuracy for 252 points.

Model	MSE (e-05)	RMSE (e-03)	MAE (e-03)	MAPE	DM test mse	P-value mae DM	DM test mae	P-value mae DM2	VaR 10 days
EWMA MSE	14,1142	11,8803	7,7360	43,3397	0,4295	0,6679	3,6767	0,0002	0,2544
EWMA MAE	13,8962	11,7882	7,5838	41,6260	0,1543	0,8774	3,2005	0,0015	0,2544
HAR MSE	13,7309	11,7178	8,2606	53,1560	-0,0507	0,9595	5,5384	<e-08	0,1533
HAR MAE	13,6397	11,6789	8,2126	52,9801	-0,1722	0,8633	5,5707	<e-08	0,1533
HAR	13,6397	11,6789	8,2126	52,9801	-0,1722	0,8633	5,5707	<e-08	0,1533
Last Values	17,9422	13,3948	7,6268	37,4586	2,3131	0,0215	1,7587	0,0798	0,1383
ARIMA	14,5067	12,0444	7,4324	40,7973	8,7439	<e-08	12,052	<e-08	0,1986
GARCH	79,9334	28,2725	13,720	82,4810	1,6996	0,0904	4,6902	<e-08	0,2040
GJR-GARCH	48,6597	22,0589	11,716	70,0866	1,4385	0,1515	4,1625	<e-08	0,1728
LSTM standart	19,9589	14,1276	9,0725	56,4351	4,7601	<e-08	6,7555	<e-08	0,1196
LSTM window	13,0910	11,4416	6,8530	35,8922	***	***	***	***	0,1280

Table 7. Dell-stock, out-of-sample test, 1-step ahead forecast, accuracy for 252 points.

Model	Description	Parameters	MSE (e-05)	RMSE (e-03)	MAE (e-03)	MAPE
EWMA MSE	alpha	0,47	5,2788	7,2655	4,3799	23,4852
EWMA MAE	alpha	0,68	5,3919	7,3429	4,3239	23,1228
HAR MSE	d,w,m:	1, 18, 110	4,9344	7,0245	4,5127	25,9045
HAR MAE	d,w,m:	1, 5, 90	4,9545	7,0388	4,4422	25,7425
HAR	d,w,m:	1, 5, 22	4,9786	7,0559	4,5514	26,3321
Last Values	–	–	5,9809	7,7336	4,4127	23,6452
ARIMA	(p,d,q):	(2, 1, 1)	5,9117	7,6887	4,4555	24,1799
GARCH	order	1,1	39,787	19,946	14,889	117,575
GJR-GARCH	order	1,1	57,082	23,891	16,530	131,826
LSTM standart	–	–	5,5212	7,4304	4,9758	31,4461
LSTM window	window	5	5,1575	7,1816	4,1140	21,5335

Table 8. CBS-stock, validation-dataset, 1-step ahead forecast, accuracy for 252 points.

Model	MSE (e-05)	RMSE (e-03)	MAE (e-03)	MAPE	DM test mse	P-value mae DM	DM test mae	P-value mae DM2	VaR 10 days
EWMA MSE	5,4257	7,3659	4,0731	28,2613	1,9592	0,0511	4,7255	<e-08	0,1823
EWMA MAE	6,0125	7,7540	4,2026	28,9532	2,0654	0,0399	4,2137	<e-08	0,1823
HAR MSE	4,9112	7,0080	4,2817	32,6479	0,4443	0,6571	6,9144	<e-08	0,1005
HAR MAE	4,9105	7,0075	4,2741	32,4164	0,4393	0,6607	6,3272	<e-08	0,1012
HAR	4,8683	6,9773	4,2497	32,2813	0,3093	0,7573	6,6897	<e-08	0,1006
Last Values	7,4220	8,6151	4,3838	30,3146	2,1572	0,0319	3,5024	0,0005	0,0935
ARIMA	6,1629	7,8504	4,4167	32,9735	3,9671	0,0000	8,6805	<e-08	0,1250
GARCH	14,151	11,895	10,280	92,2075	7,1467	<e-08	14,922	<e-08	0,1584
GJR-GARCH	15,325	12,379	10,436	92,8045	6,8824	<e-08	14,636	<e-08	0,1587
LSTM standart	5,0528	7,1083	4,6181	36,6197	0,7158	0,4747	7,8448	<e-08	0,1054
LSTM window	4,7921	6,9225	3,2768	20,2920	***	***	***	***	0,0829

Table 9. CBS-stock, out-of-sample test, 1-step ahead forecast, accuracy for 252 points.

Model	Description	Parameters	MSE (e-05)	RMSE (e-03)	MAE (e-03)	MAPE
EWMA MSE	alpha	0,2	41,8744	20,4632	9,3206	23,2058
EWMA MAE	alpha	0,28	42,2200	20,5475	9,2023	22,5636
HAR MSE	d,w,m:	3, 4, 55	40,7741	20,1926	8,5367	20,7522
HAR MAE	d,w,m:	3, 15, 30	40,9492	20,2359	8,4996	20,4421
HAR	d,w,m:	1, 5, 22	45,3501	21,2955	8,9237	20,7829
Last Values	–	–	64,2884	25,3551	10,872	25,7694
ARIMA	(p,d,q):	(1, 1, 1)	54,0468	23,2479	10,147	24,5666
GARCH	order	1,1	82,8823	28,7892	23,970	72,8169
GJR-GARCH	order	1,1	83,2874	28,8595	23,847	71,8954
LSTM standart	–	–	46,8581	22,2736	26,547	66,4353
LSTM window	window	12	42,5604	20,6301	8,6655	20,6121

Table 10. S&P 500, validation-dataset, 1-step ahead forecast, accuracy for 245 points.

Model	MSE (e-05)	RMSE (e-03)	MAE (e-03)	MAPE	DM test mse	P-value mae DM	DM test mae	P-value mae DM2	VaR 10 days
EWMA MSE	51,7004	22,7377	14,8143	32,0655	3,4105	0,0007	4,3333	<e-08	0,2807
EWMA MAE	47,6968	21,8396	14,0323	30,1342	2,9263	0,0037	2,7277	0,0068	0,2805
HAR MSE	49,4088	22,2281	13,4078	28,1917	2,2882	0,0229	1,7231	0,0861	0,3185
HAR MAE	49,1897	22,1787	13,2569	27,3338	2,2819	0,0233	1,3088	0,1918	0,3177
HAR	45,0559	21,2263	12,7762	26,790	2,5911	0,0101	-0,3437	0,7313	0,3185
Last Values	43,1101	20,7629	14,2981	30,7739	0,2095	0,8341	2,2326	0,0264	0,3525
ARIMA	46,1339	21,4788	14,1858	30,8716	3,0891	0,0022	6,0096	<e-08	0,2823
GARCH	174,268	41,7454	34,1938	71,0463	9,5905	<e-08	18,972	<e-08	0,1040
GJR-GARCH	175,741	41,9215	34,5954	71,9429	9,6029	<e-08	19,613	<e-08	0,1046
LSTM standart	48,7022	23,5619	14,4471	32,9160	3,4729	<e-08	12,181	<e-08	0,1511
LSTM window	41,6775	20,4150	12,8474	28,505	***	***	***	***	0,3374

Table 11. S&P 500-index, out-of-sample test, 1-step ahead forecast, accuracy for 245 points.

Model	Description	Parameters	MSE (e-05)	RMSE (e-03)	MAE (e-03)	MAPE
EWMA MSE	alpha	0,42	17,3251	13,1625	7,9259	21,6890
EWMA MAE	alpha	0,83	19,5003	13,9643	7,6130	21,1396
HAR MSE	d,w,m:	1, 5, 45	17,2831	13,1465	8,9144	29,9428
HAR MAE	d,w,m:	1, 4, 18	17,4985	13,2281	8,7833	29,1916
HAR	d,w,m:	1, 5, 22	17,4095	13,1945	8,8089	29,3820
Last Values	–	–	21,3450	14,6099	7,8045	21,8513
ARIMA	(p,d,q):	(3, 1, 3)	25,0838	15,8378	8,5929	23,2321
GARCH	order	1,1	3348,44	182,987	145,84	718,887
GJR-GARCH	order	1,1	3115,92	176,519	137,70	687,079
LSTM standart	–	–	24,8242	15,7557	9,4235	23,9942
LSTM window	window	8	16,3256	12,7771	7,2293	21,0681

Table 12. Bitcoin-USD, validation-dataset, 1-step ahead forecast, accuracy for 252 points.

Model	MSE (e-05)	RMSE (e-03)	MAE (e-03)	MAPE	DM test mse	P-value mae DM	DM test mae	P-value mae DM2	VaR 10 days
EWMA MSE	27,7132	16,6472	8,3999	20,6981	1,4792	0,1403	1,8250	0,0691	0,3956
EWMA MAE	28,5206	16,8880	8,7378	21,7385	0,6404	0,5224	2,0189	0,0445	0,3956
HAR MSE	25,8854	16,0889	9,0112	25,4136	1,3917	0,1652	5,5401	<e-08	0,2805
HAR MAE	25,8716	16,0846	8,9371	25,1927	1,2148	0,2255	5,2337	<e-08	0,2793
HAR	26,1071	16,1576	8,9817	25,2597	1,6145	0,1076	5,6381	<e-08	0,2795
Last Values	29,8399	17,2742	8,9527	22,7036	0,6609	0,5092	2,0390	0,0424	0,2604
ARIMA	38,7652	19,6889	9,6716	23,0919	3,7090	0,0002	7,6181	<e-08	0,2598
GARCH	11810,2	343,660	176,07	403,906	3,8704	0,0001	9,2925	<e-08	1,5557
GJR-GARCH	13071,7	361,548	180,61	409,336	3,7308	0,0002	8,9830	<e-08	1,5891
LSTM standart	50,4766	22,4670	15,245	40,6017	4,0497	0,0001	13,873	<e-08	0,1493
LSTM window	24,4282	15,6290	7,8785	20,3574	***	***	***	***	0,2583

Table 13. Bitcoin-USD, out-of-sample test, 1-step ahead forecast, accuracy for 252 points.

Model	Description	Parameters	MSE (e-05)	RMSE (e-03)	MAE (e-03)	MAPE
EWMA MSE	alpha	0,5	7,2411	8,5095	5,7709	22,5619
EWMA MAE	alpha	0,7	7,4220	8,6151	5,6981	22,3058
HAR MSE	d,w,m:	1, 5, 30	6,9555	8,3400	6,1236	26,7363
HAR MAE	d,w,m:	1, 4, 24	8,1742	9,0411	6,0497	22,9636
HAR	d,w,m:	1, 5, 22	6,9657	8,3460	6,1170	26,7087
Last Values	–	–	8,2490	9,0824	5,9349	23,2643
ARIMA	(p,d,q):	(1, 1, 2)	7,4762	8,6465	5,7329	22,8089
GARCH	order	1,1	1003,9	100,19	60,207	284,042
GJR-GARCH	order	1,1	921,15	95,977	59,829	287,266
LSTM standart	–	–	24,642	15,698	11,812	40,9822
LSTM window	window	7	6,7176	8,1961	5,5248	22,8914

Table 14. Ethereum-USD, validation-dataset, 1-step ahead forecast, accuracy for 252 points.

Model	MSE (e-05)	RMSE (e-03)	MAE (e-03)	MAPE	DM test mse	P-value mae DM	DM test mae	P-value mae DM2	VaR 10 days
EWMA MSE	14,5095	12,0455	6,4798	26,0383	0,6170	0,5377	1,6013	0,1105	0,2472
EWMA MAE	15,1958	12,3271	6,6222	26,8891	0,5746	0,5660	1,8285	0,0686	0,2469
HAR MSE	13,1807	11,4807	6,6540	29,3306	-0,2493	0,8033	2,2370	0,0261	0,1787
HAR MAE	14,7789	12,1568	7,1052	31,6274	0,7861	0,4325	3,0047	0,0029	0,1813
HAR	13,1785	11,4797	6,6583	29,3342	-0,2573	0,7971	2,2608	0,0246	0,1787
Last Values	16,6921	12,9198	6,9548	28,7158	0,7582	0,4490	2,1630	0,0314	0,1683
ARIMA	15,1794	12,3204	7,3057	31,4821	2,7745	0,0059	7,1878	<e-08	0,1801
GARCH	584,465	76,4503	54,010	239,247	4,6473	<e-08	14,769	<e-08	0,5650
GJR-GARCH	513,573	71,6640	51,818	229,280	5,0685	<e-08	15,610	<e-08	0,5489
LSTM standart	27,5347	16,5935	10,357	37,0491	3,1206	0,0020	10,646	<e-08	0,0946
LSTM window	13,5033	11,6203	6,0079	22,6919	***	***	***	***	0,1461

Table 15. Ethereum-USD, out-of-sample test, 1-step ahead forecast, accuracy for 252 points.

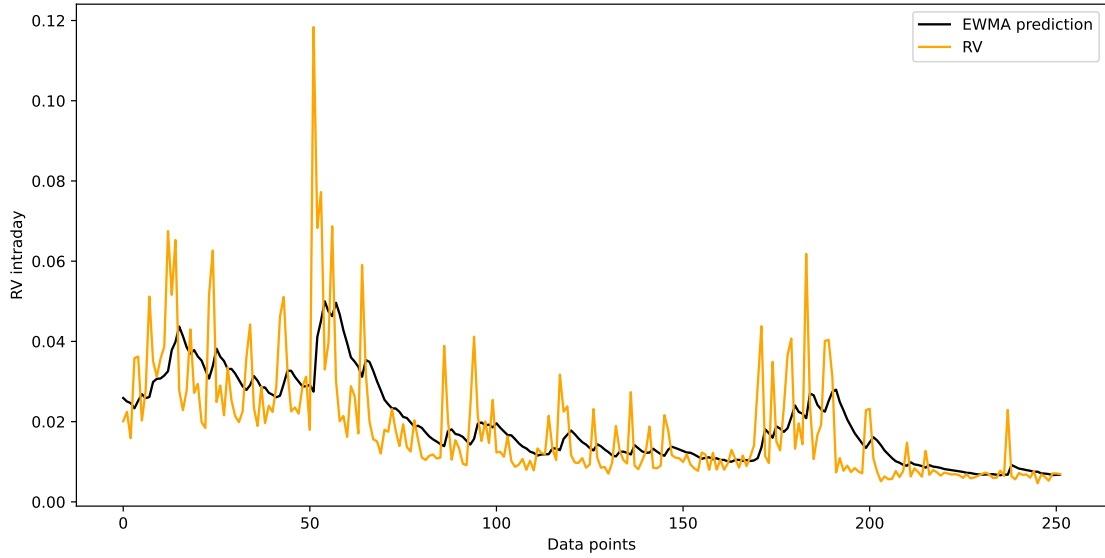


Figure 2. EWMA-model prediction for Dell stock

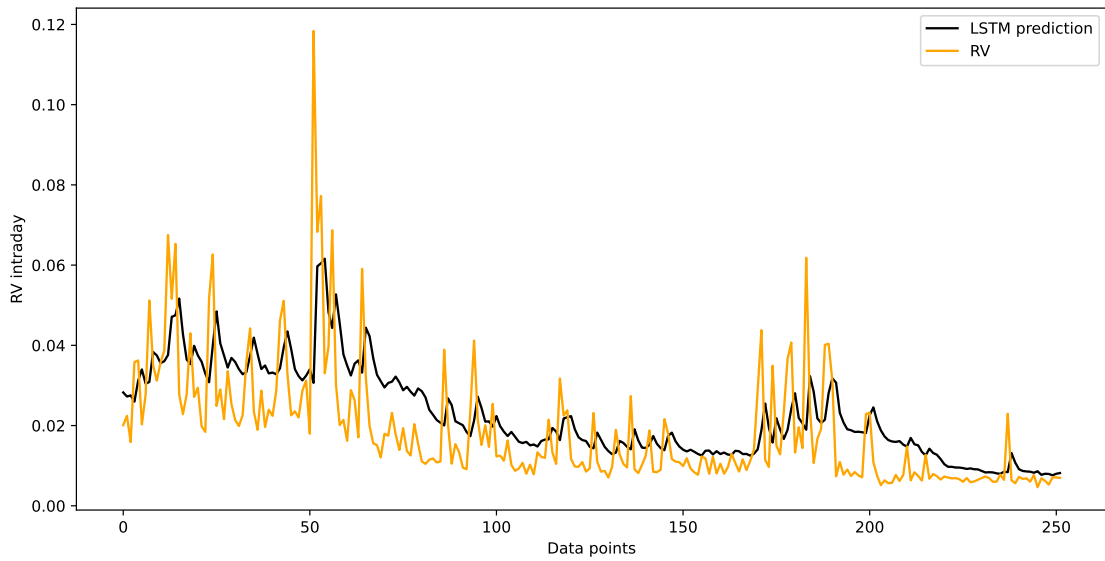


Figure 3. Long Short-Term Memory RNN prediction for Dell stock

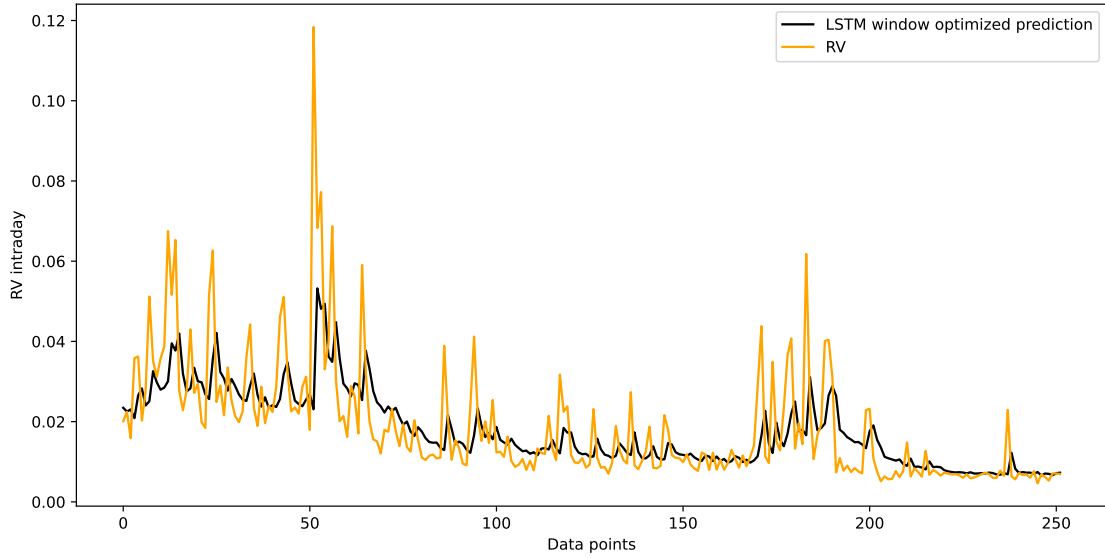


Figure 4. Long Short-Term Memory RNN with opt.window prediction for Dell stock

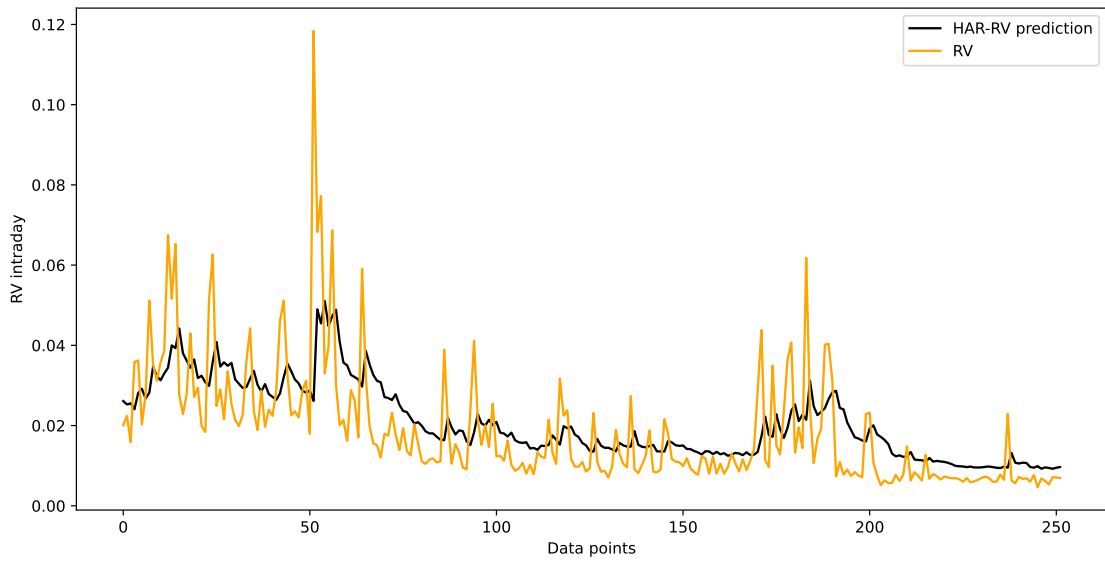


Figure 5. Heterogenous Autoregressive Realized Volatility Model prediction for Dell stock

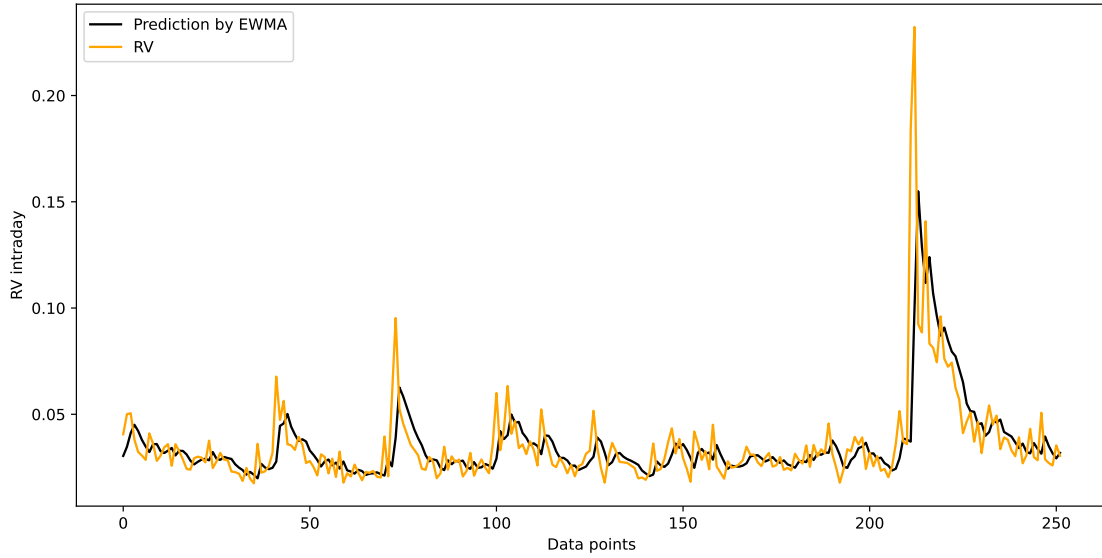


Figure 6. EWMA model prediction for Bitcoin cryptocurrency

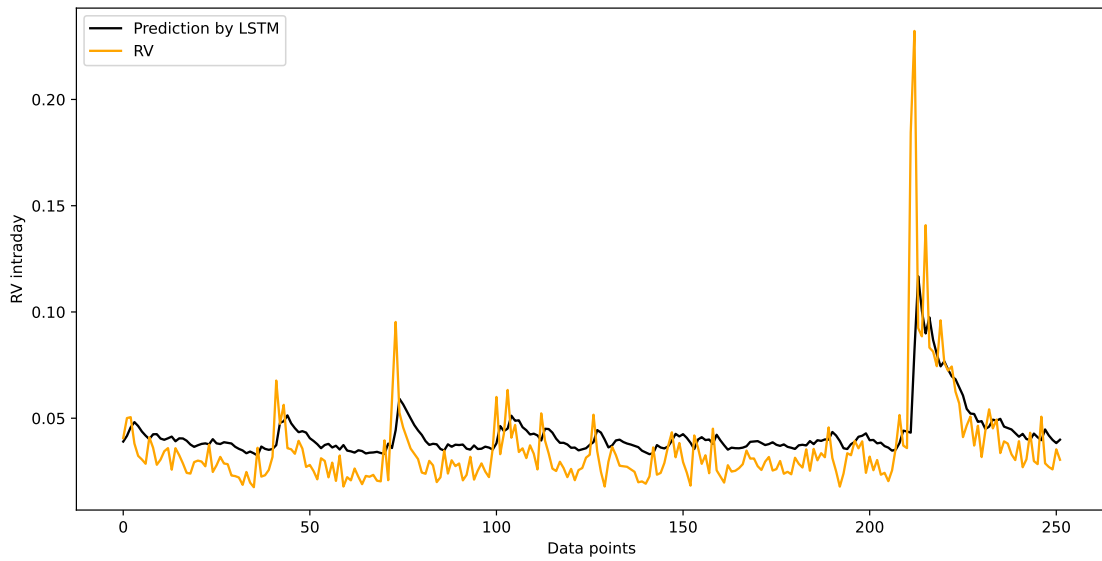


Figure 7. Long Short-Term Memory RNN prediction for Bitcoin cryptocurrency

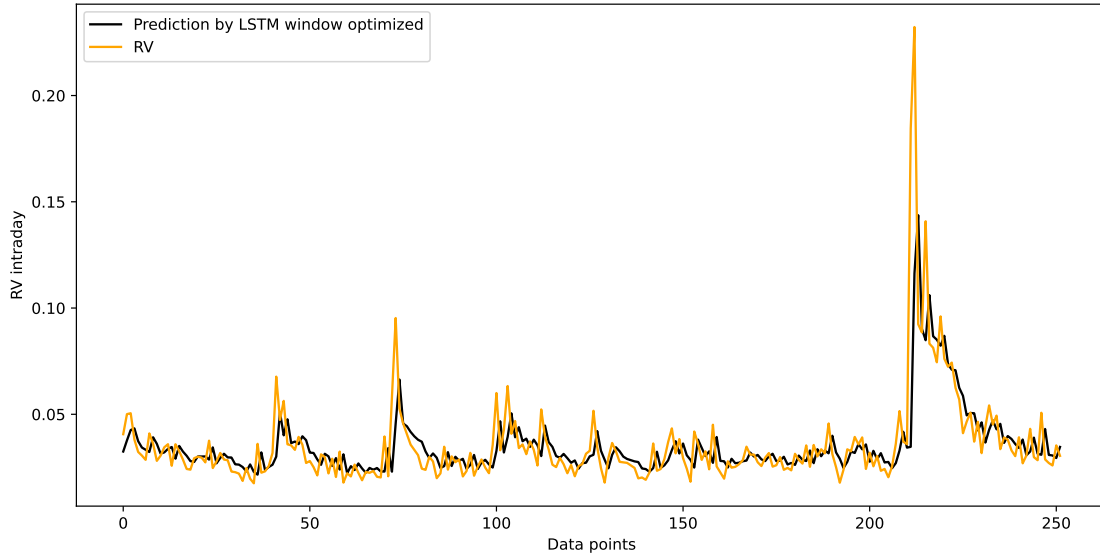


Figure 8. Long Short-Term Memory RNN with opt.window prediction for Bitcoin cryptocurrency

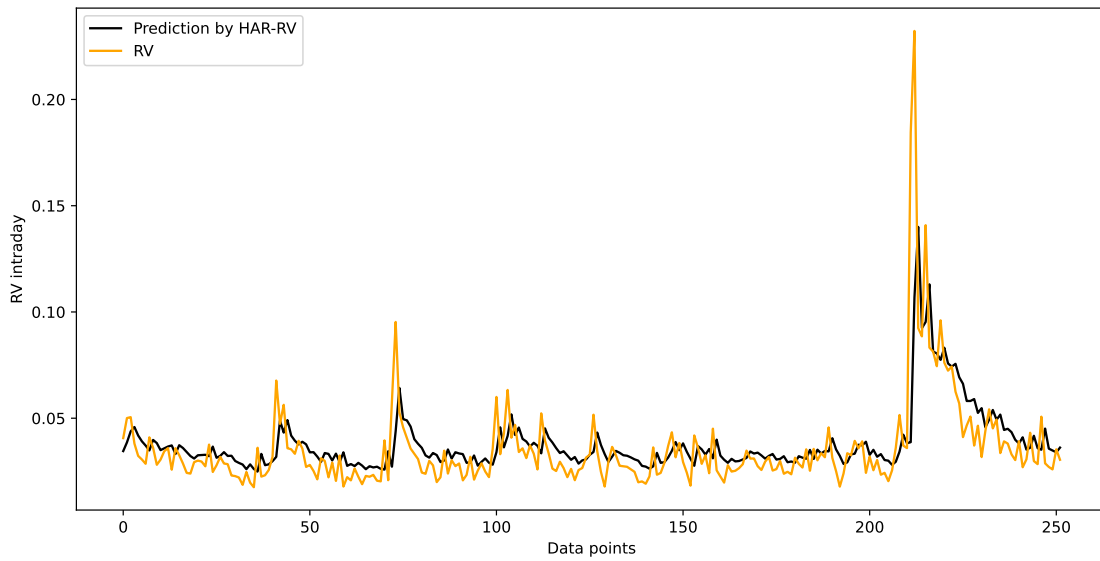


Figure 9. Heterogenous Autoregressive Realized Volatility Model prediction for Bitcoin cryptocurrency

References

1. Bachelier, L. Théorie de la spéculation. In *Annales scientifiques de l'École normale supérieure*, vol. 17, 21–86 (1900).
2. Jarrow, R., Protter, P. *et al.* A short history of stochastic integration and mathematical finance: The early years, 1880–1970. In *A festschrift for Herman Rubin*, 75–91 (Institute of Mathematical Statistics, 2004).
3. Cont, R. Empirical properties of asset returns: stylized facts and statistical issues. *Quant. finance* **1**, 223 (2001).
4. Engle, R. F. Autoregressive conditional heteroscedasticity with estimates of the variance of united kingdom inflation. *Econom. J. econometric society* 987–1007 (1982).
5. Bollerslev, T. Generalized autoregressive conditional heteroskedasticity. *J. econometrics* **31**, 307–327 (1986).
6. Poon, S.-H. & Granger, C. W. Forecasting volatility in financial markets: A review. *J. economic literature* **41**, 478–539 (2003).
7. Ghysels, E., Harvey, A. C. & Renault, E. 5 stochastic volatility. *Handb. statistics* **14**, 119–191 (1996).
8. Pagan, A. R. & Schwert, G. W. Alternative models for conditional stock volatility. *J. econometrics* **45**, 267–290 (1990).
9. West, K. D. & Cho, D. The predictive ability of several models of exchange rate volatility. *J. econometrics* **69**, 367–391 (1995).
10. Khan, M. A. I. Financial volatility forecasting by nonlinear support vector machine heterogeneous autoregressive model: evidence from nikkei 225 stock index. *Int. J. Econ. Finance* **3**, 138 (2011).
11. Bucci, A. Realized volatility forecasting with neural networks. *J. Financial Econom.* **18**, 502–531 (2020).
12. Arnerić, J., Poklepović, T. & Aljinović, Z. Garch based artificial neural networks in forecasting conditional variance of stock returns. *Croat. Oper. Res. Rev.* 329–343 (2014).
13. Clements, M. P. & Krolzig, H.-M. A comparison of the forecast performance of markov-switching and threshold autoregressive models of us gnp. *The Econom. J.* **1**, 47–75 (1998).
14. Pavlidis, E., Paya, I., Peel, D. *et al.* A new test for rational speculative bubbles using forward exchange rates: The case of the interwar german hyperinflation. *Dep. Econ. Lancaster university Manag. school, UK* (2012).
15. Vortelinos, D. I. Forecasting realized volatility: Har against principal components combining, neural networks and garch. *Res. international business finance* **39**, 824–839 (2017).
16. Bucci, A. *et al.* Forecasting realized volatility: a review. *J. Adv. Stud. Finance (JASF)* **8**, 94–138 (2017).
17. Miura, R., Pichl, L. & Kaizoji, T. Artificial neural networks for realized volatility prediction in cryptocurrency time series. In *International Symposium on Neural Networks*, 165–172 (Springer, 2019).
18. Rosa, R., Maciel, L., Gomide, F. & Ballini, R. Evolving hybrid neural fuzzy network for realized volatility forecasting with jumps. In *2014 IEEE Conference on Computational Intelligence for Financial Engineering & Economics (CIFEr)*, 481–488 (IEEE, 2014).
19. Hamid, S. A. & Iqbal, Z. Using neural networks for forecasting volatility of s&p 500 index futures prices. *J. Bus. Res.* **57**, 1116–1125 (2004).
20. Black, F. The pricing of commodity contracts. *J. financial economics* **3**, 167–179 (1976).
21. Nelson, D. B. Stationarity and persistence in the garch (1, 1) model. *Econom. theory* **6**, 318–334 (1990).
22. Hochreiter, S. & Schmidhuber, J. Long short-term memory. *Neural computation* **9**, 1735–1780 (1997).
23. Cho, K. *et al.* Learning phrase representations using rnn encoder-decoder for statistical machine translation. *arXiv preprint arXiv:1406.1078* (2014).
24. Hull, J. & White, A. The pricing of options on assets with stochastic volatilities. *The journal finance* **42**, 281–300 (1987).
25. Mandelbrot, B. The variation of some other speculative prices. *The J. Bus.* **40**, 393–413 (1967).
26. Barndorff-Nielsen, O. E. & Shephard, N. Econometric analysis of realized volatility and its use in estimating stochastic volatility models. *J. Royal Stat. Soc. Ser. B (Statistical Methodol.* **64**, 253–280 (2002).
27. Barndorff-Nielsen, O. E. & Shephard, N. Estimating quadratic variation using realized variance. *J. Appl. econometrics* **17**, 457–477 (2002).
28. Fama, E. F. The behavior of stock-market prices. *The journal Bus.* **38**, 34–105 (1965).

29. Perry, T. L., Godin, D. V. & Hansen, S. Parkinson's disease: a disorder due to nigral glutathione deficiency? *Neurosci. letters* **33**, 305–310 (1982).
30. Ding, Z., Granger, C. W. & Engle, R. F. A long memory property of stock market returns and a new model. *J. empirical finance* **1**, 83–106 (1993).
31. Diebold, F. X. *Elements of forecasting* (Citeseer, 1998).
32. Atkins, A., Niranjana, M. & Gerding, E. Financial news predicts stock market volatility better than close price. *The J. Finance Data Sci.* **4**, 120–137 (2018).
33. Mastro, D. Forecasting realized volatility: Arch-type models vs. the har-rv model. *Available at SSRN 2519107* (2014).
34. Nelson, D. B. Conditional heteroskedasticity in asset returns: A new approach. *Econom. J. Econom. Soc.* 347–370 (1991).
35. Glosten, L. R., Jagannathan, R. & Runkle, D. E. On the relation between the expected value and the volatility of the nominal excess return on stocks. *The journal finance* **48**, 1779–1801 (1993).
36. Zakoian, J.-M. Threshold heteroskedastic models. *J. Econ. Dyn. control* **18**, 931–955 (1994).
37. Jafari, G., Bahraminasab, A. & Norouzzadeh, P. Why does the standard garch (1, 1) model work well? *Int. J. modern physics C* **18**, 1223–1230 (2007).
38. Hansen, P. R. A test for superior predictive ability. *J. Bus. & Econ. Stat.* **23**, 365–380 (2005).
39. Brockwell, P., Chadraa, E. & Lindner, A. Continuous-time garch processes. *The Annals Appl. Probab.* **16**, 790–826 (2006).
40. Corsi, F. A simple approximate long-memory model of realized volatility. *J. Financial Econom.* **7**, 174–196 (2009).
41. Müller, U. A. *et al.* Fractals and intrinsic time: A challenge to econometricians. *Unpubl. manuscript, Olsen & Assoc. Zürich* 130 (1993).
42. Corsi, F., Audrino, F. & Renó, R. Har modeling for realized volatility forecasting. - (2012).
43. Box, G. E., Jenkins, G. M., Reinsel, G. C. & Ljung, G. M. *Time series analysis: forecasting and control* (John Wiley & Sons, 2015).
44. Olah, C. Understanding lstm networks. <https://colah.github.io/posts/2015-08-Understanding-LSTMs/> (2015).
45. Cho, K. *et al.* Learning phrase representations using rnn encoder-decoder for statistical machine translation. *arXiv preprint arXiv:1406.1078* (2014).
46. Panchal, G., Ganatra, A., Kosta, Y. & Panchal, D. Searching most efficient neural network architecture using akaike's information criterion (aic). *Int. J. Comput. Appl.* **1**, 41–44 (2010).
47. Diebold, F. X. Comparing predictive accuracy, twenty years later: A personal perspective on the use and abuse of diebold–mariano tests. *J. Bus. & Econ. Stat.* **33**, 1–1 (2015).
48. Harvey, D., Leybourne, S. & Newbold, P. Testing the equality of prediction mean squared errors. *Int. J. forecasting* **13**, 281–291 (1997).
49. Jorion, P. Value at risk. - (2000).
50. Laptev, N., Yosinski, J., Li, L. E. & Smyl, S. Time-series extreme event forecasting with neural networks at uber. In *International conference on machine learning*, vol. 34, 1–5 (2017).
51. Chollet, F. *Deep learning with Python* (Simon and Schuster, 2017).
52. Burnham, K. P. & Anderson, D. R. Multimodel inference: understanding aic and bic in model selection. *Sociol. methods & research* **33**, 261–304 (2004).